Synthesis and Biological Evaluation of Novel Tetrahydro-β-carboline Derivatives as Antitumor Growth and Metastasis Agents through Inhibiting the Transforming Growth Factor-β Signal...

ARTICLE *in* JOURNAL OF MEDICINAL CHEMISTRY · JANUARY 2014

Impact Factor: 5.45 · DOI: 10.1021/jm401117t · Source: PubMed

Journal of Medicinal Chemistry

Article

pubs.acs.org/jmc

Synthesis and Biological Evaluation of Novel Tetrahydro-β-carboline Derivatives as Antitumor Growth and Metastasis Agents through Inhibiting the Transforming Growth Factor-β Signaling Pathway

Cong Zheng,[†,#] Yuanzhang Fang,[†,#] Weiguang Tong,[†] Guoliang Li,[†] Haigang Wu,[†] Wenbo Zhou,[†] Qingxiang Lin,[†] Feifei Yang,[†] Zhengfeng Yang,[†] Peng Wang,[†] Yangrui Peng,[†] Xiufeng Pang,[†] Zhengfang Yi,[†] Jian Luo,*[,†] Mingyao Liu,*[,†,‡] and Yihua Chen*[,†]

[†]Shanghai Key Laboratory of Regulatory Biology, The Institute of Biomedical Sciences and School of Life Sciences, East China Normal University, Shanghai 200241, China

[‡]Center for Cancer and Stem Cell Biology, Institute of Biosciences and Technology, Texas A&M University Health Science Center, Houston, Texas 77030, United States

Supporting Information

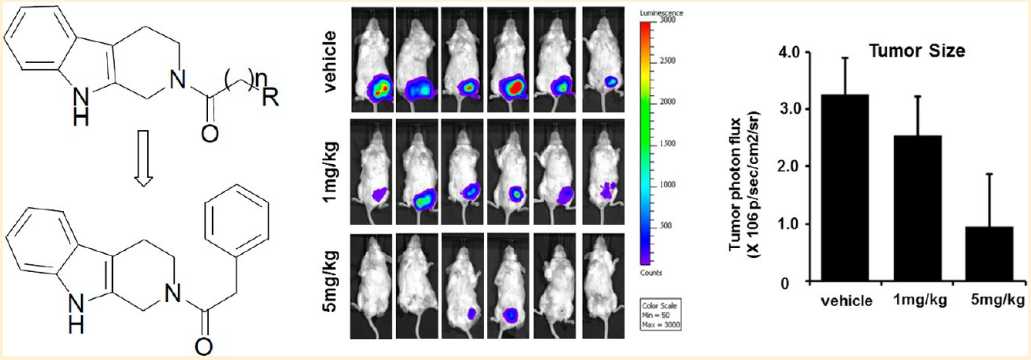

ABSTRACT: The transforming growth factor beta (TGFβ) signaling cascade is considered as one of the pivotal oncogenic pathways in most advanced cancers. Inhibition of the TGFβ signaling pathway by specific antagonists, neutralizing antibodies, or small molecules is considered as an effective strategy for the treatment of tumor growth and metastasis. Here we demonstrated the identification of a series of tetrahydro-β-carboline derivatives from virtual screening which potentially inhibit the TGFβ signaling pathway. Optimization of the initial hit compound 2-benzoyl-1,3,4,9-tetrahydro-β-carboline (**8a**) through substitution at different positions to define the structure−activity relationship resulted in the discovery of potent inhibitors of the TGFβ signaling pathway. Among them, compound **8d**, one of the tested compounds, not only showed potent inhibition of lung cancer cell proliferation and migration in vitro but also strongly suppressed growth of lung cancer and breast cancer in vivo.

INTRODUCTION

Cancer is currently a worldwide public health problem, accounting for 23% of all deaths and second only to heart diseases.[1] More than 1.6 million new cancer cases and 577 000 deaths from cancer were estimated to occur in the United States in 2012.[2] Tumor metastasis is the most common cause of cancer related-death, accounting for about 90% of the mortality from solid tumors.[3,4] Epithelial−mesenchymal transition (EMT) is well-recognized as one of the crucial factors contributing to tumor metastasis, which may be induced by transforming growth factor-β (TGFβ) as well as other signal transduction pathways.[5] TGFβ is a cytokine that plays pivotal roles in regulating cell proliferation, differentiation, migration, adhesion, and immune response.[6] The deregulation of TGFβ signaling has been implicated in the pathogenesis of various diseases, including fibrosis,[7] atherosclerosis,[8] and cancer.[9] More importantly, the TGFβ signaling pathway is considered as one of the pivotal oncogenic factors in advanced cancer based on a variety of clinical evidence,[10] Given the key role of TGFβ in regulating the EMT process and tumor progression,[11−13] consequently, blocking the TGFβ signal transduction pathway has been considered an attractive approach for the development of cancer therapeutics that simultaneously suppress tumor growth and metastasis while restoring the tumor microenvironment.

Previous studies reported that many antibodies and small-molecule inhibitors,[14−17] such as **1** (LY-2157229),[18] **2** (SD-208),[3,19] **3** (SB-431542),[5,20] **4** (SB-505124),[21] **5** (GW-6604),[22] and **6** (SM-16)[23](Figure 1), were developed through targeting aspects of the TGFβ signaling pathway such as autophosphorylation of transforming growth factor-β receptor type I (TGFβRI) and TGFβ-induced transcription of matrix genes in reporter assays at

Received: July 24, 2013
Published: January 13, 2014

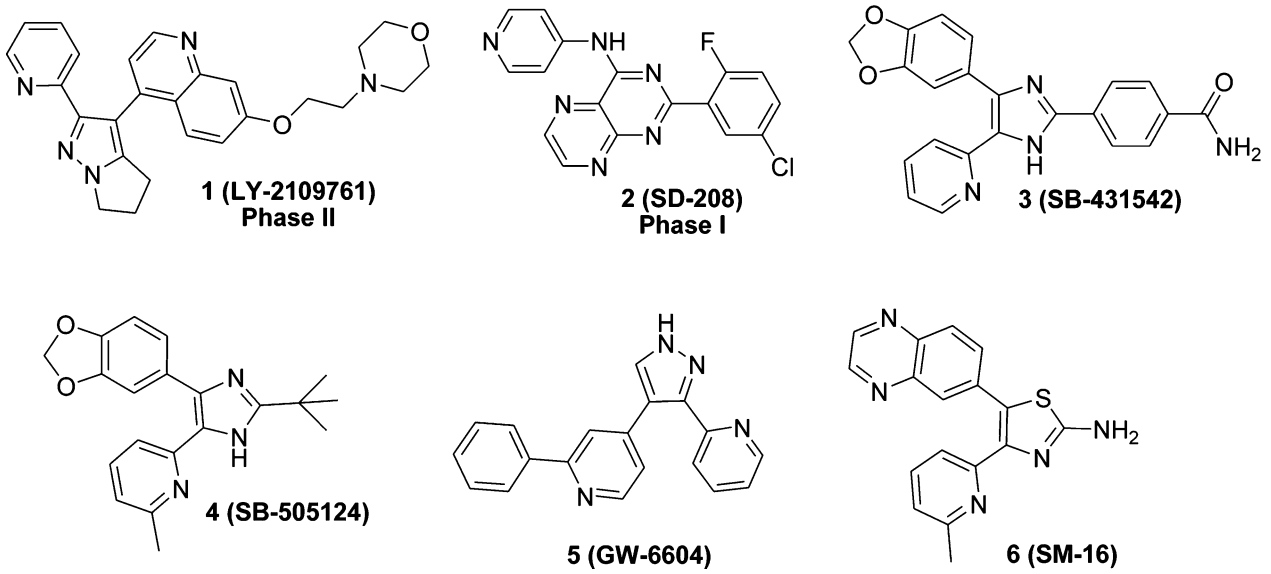

Figure 1. Chemical structures of several known TGFβRI kinase inhibitors.

submicromolar concentrations.[24] More importantly, several candidates have been advanced into phase III clinical trials for the treatment of a number of diseases, particularly fibrosis and cancer.[17] To date, most of the known small molecular TGFβRI kinase inhibitors are five-membered heterocyclic chemotypes.[25] To identify more novel scaffolds of TGFβRI kinase inhibitor candidates, a virtual screening program was carried out using a docking model of TGFβRI (PDB ID: 3TZM) interaction with a chemical database containing more than 400 000 small molecules derived from ChemDiv (www.chemdiv.com) as well as from our laboratory. According to the docking results, a class of tetrahydro-β-carboline derivatives, which were substantially different from known TGFβRI kinase inhibitors, was identified and subsequently developed to show potent interactions with the TGFβRI kinase domain. One of the novel tetrahydro-β-carboline derivatives, developed by our laboratory, showed highly potent inhibition of the TGFβ signaling pathway in vitro and suppressed breast cancer metastases in vivo.[26] Whether or not this type of tetrahydro-β-carboline compound inhibits the tumor growth or metastasis of other tumors remains to be determined to assess its pharmacological spectrum. In the present study, a series of novel tetrahydro-β-carboline derivatives were herein identified as potent antitumor growth and metastasis agents through regulating the TGFβ signaling pathway. Modification of the initial hit compound 2-benzoyl-1,3,4,9-tetrahydro-β-carboline with different substitutions as well as varying the linker allowed the elucidation of the structure–activity relationship, resulting in the discovery of high-affinity agents that regulate the TGFβ signaling pathway. Among the derivatives, compound **8d** not only showed potent inhibition against tumor cell proliferation and migration in vitro but also strongly suppressed tumor growth of lung cancer and breast cancer in vivo.

CHEMISTRY

Generally, compounds **8a–r** were prepared according to the methods described in Scheme 1. Commercial or synthetic acids were routinely coupled with tetrahydro-β-carboline in the presence of EDC and HOBt or other coupling reagents to generate **8a–r**. For preparing substitutions of the phenyl ring in tetrahydro-β-carbolines **9** and **10**, two procedures were carried out as listed in Schemes 2 and 3. Substituted indoles were transferred to the corresponding tryptamines according to the reported literature,[27] which then reacted with different

Scheme 1[a]

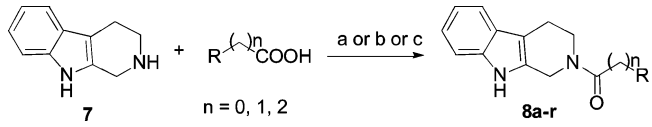

[a]Reagents and conditions: (a) EDC, HOBt, DMF, 0 °C then to rt; (b) HATU, DMF, 0 °C then to rt; (c) CDI, DMF, 0 °C then to rt.

aldehydes or diethylacetals via the Pictet–Spengler reaction to afford substituted tetrahydro-β-carbolines as the key intermediates.[27] Then the intermediates were eventually transformed to target compounds using the method listed in Scheme 1. Alternatively, substituted anilines could be converted to diazonium salts, which were then transferred to 1-oxo-tetrahydro-β-carbolines in the presence of 2-oxopiperidine-3-carboxylic acid[28] and then reduced to tetrahydro-β-carbolines with lithium aluminum hydride.[29] Finally, the intermediate carbolines were coupled with acids to afford the target compounds.

RESULTS AND DISCUSSION

Smad binding element (SBE) luciferase reporter assay, which evaluates the activity of the TGFβ signaling pathway and inhibition of cancer cell proliferation, were chosen to evaluate and confirm the potential antitumor efficacy of tetrahydro-β-carboline analogues which were derived from virtual screening and subsequent modification at the molecular and cellular level in vitro. In our preliminary data, compound **8a** was shown to have weak inhibition in a SBE luciferase reporter assay, though it was structurally different from known TGFβRI inhibitors (Table 1). Compound **8a** was then selected as a hit compound for further optimization for the purpose of increasing the anticancer potency because tetrahydro-β-carboline derivatives possessed a variety of pharmacological activities.[30] First, the terminal phenyl ring (at the right portion of the molecule) was replaced by other aromatic groups such as 2-thiopheneyl (**8b**) or 2-pyridinyl rings (**8c**, Figure 2B and Table 1), but upon testing in the SBE luciferase reporter assay, the inhibitory rate at 1.0 μM decreased, ranging from 9.5% $\pm$ 1.1% to 2.2% $\pm$ 0.1% and 1.1% $\pm$ 0.2% compared to the parent compound and indicating that retaining the phenyl ring for further

dx.doi.org/10.1021/jm401117t | J. Med. Chem. 2014, 57, 600–612

Scheme 2[a]

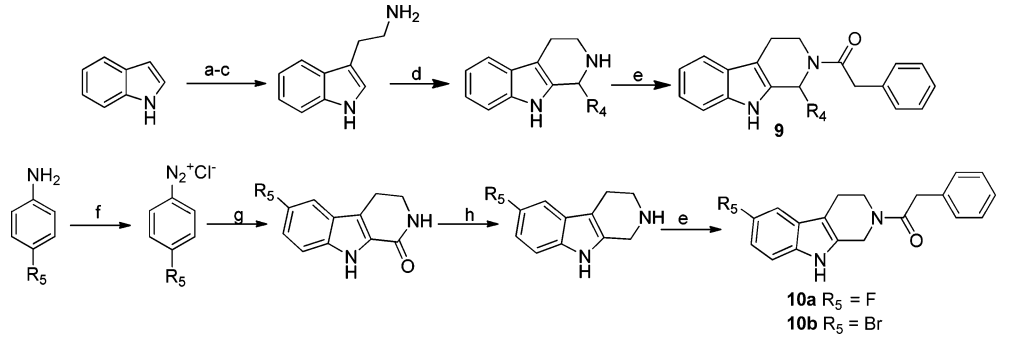

[a]Reagents and conditions: (a) $(COCl)_2$, ether, reflux; (b) $NH_3{\cdot}H_2O$, $CHCl_3$, reflux; (c) $LiAlH_4$, THF, reflux; (d) AcOH, reflux or 5% TFA/DCM, 0 °C then to rt; (e) EDC, HOBt, DMF, 0 °C then to rt; (f) $NaNO_2$, concd HCl, 0 °C; (g) HCOOH, rt; (h) $LiAlH_4$, 1,4-dioxane, reflux.

Scheme 3[a]

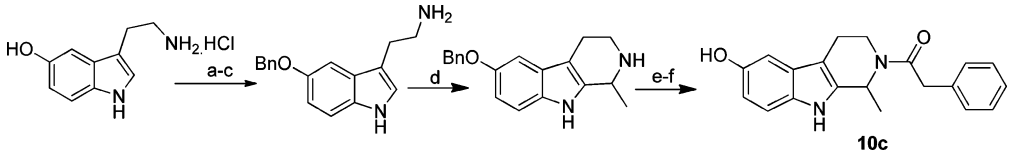

[a]Reagents and conditions: (a) $(Boc)_2O$, Et_3N, 1, 4-dioxane, rt; (b) BnBr, K_2CO_3, DMF, 0 °C then to rt; (c) TFA, DCM, 0 °C then to rt; (d) CH_3CHO, AcOH, 85 °C; (e) EDC, HOBt, DMF, 0 °C then to rt; (f) H_2, 10% Pd/C, MeOH, rt.

Table 1. Effect of Aromatic Group Substitutions against SBE Luciferase Reporter Gene Expression Inhibition and PC-9 Cell Proliferation

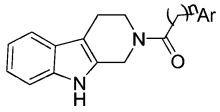

compd. no.	n	Ar	% SBE luciferase inhibition rate (1.0 μM)	% PC-9 cell proliferation inhibition rate (10.0 μM)
8a	0	phenyl	9.5 ± 1.1	7
8b	0	2-thiophenyl	2.2 ± 0.1	9
8c	0	2-pyridinyl	1.1 ± 0.2	4
8d	1	phenyl	72.4 ± 7.1	59
8e	2	phenyl	31.1 ± 2.9	48

optimization would be more suitable. Second, the length of the linker between tetrahydro-β-carboline and the terminal aromatic group was explored, as shown in Figure 2B. We found that the length of linker dramatically influenced the inhibitory activity; for example, the activity of compounds **8a,d,e** showed a parabolic tendency, i.e., varying n = 0 to n = 2, the SBE luciferase inhibitory rate was 9.5% ± 1.1%, 72.4% ± 7.1%, and 31.1% ± 2.9% (Table 1). Accordingly, the lung cancer cell (PC-9) proliferation rate was inhibited by 0%, 59%, and 48%, respectively, when incubated with a 10.0 μM concentration of compounds (**8a,d,e**). The trend suggests that phenylacetyl substitution in this position was more suitable, which was also supported when R_2 was a Boc-protected amine (**8f,g**). These compounds showed an SBE luciferase inhibition rate of 58.8% ± 5.9% and 44.3% ± 1.9% when n = 0 and n = 1 at 1.0 μM, respectively. The inhibition of PC-9 lung cancer cell proliferation was 31% and 0% when incubated with compounds (**8f,g**) at 10.0 μM concentration. These data indicated that a suitable linker was important for SBE luciferase inhibition and anticancer cell proliferation. Thus, compound **8d** was chosen for further optimization based on evaluating the SAR in greater detail.

As shown in Figure 2 and Table 2, to explore the effect of substitution in the linker, a few substituents (R_2) were next introduced to the methylene group of the compound **8d** linker, such as a hydroxyl group (**8h**), an amino group (**8i**), BocNH (**8f**), and a hydroxylphenyl group (**8j**); unfortunately, all of these substitutions resulted in a decrease in SBE luciferase inhibitory activity as well as less tumor cell proliferation inhibition, suggesting that more simple substitutions might be more effective for increasing or retaining inhibitory activity against PC-9 cell proliferation.

Compounds containing a hydrophobic domain as well as a hydrophilic domain near the position of the terminal phenyl group of aryl tetrahydro-β-carboline derivatives were predicted to have higher efficacy in our docking model analysis (Figure S1, Supporting Information). This suggested that modifications of the terminal phenyl group were very attractive for analyzing the SAR. Therefore, in addition to examining different linkers and diverse heteroaromatic substitutions on the terminal parts of tetrahydro-β-carboline, we also focused on exploring the effects of different phenyl substitutions on SBE luciferase inhibition as well as on cancer cell proliferation First, the substitution position of the terminal phenyl group was explored, in which *o*-, *m*-, and *p*-hydroxyl groups (**8k**−**m**, Table 3) were synthesized. The results demonstrated that the activity of para-position substitution was superior to meta-position or ortho-position (**8m** > **8l** > **8k**). The inhibitory rates were 62.4%, 29.1%, and 19.7% respectively, at 1.0 μM. However, dual substitution in both the meta- and para-position did not improve the inhibition activity compared to a single substitution (**8n** vs **8m** or **8l**). Further modification was focused on substitutions in the para-position of the phenyl ring. Shortly afterward we synthesized a series of derivatives with phenyl ring para-position substitution to discover more potent compounds (Table 3). We explored substitutions with diverse electronic properties, such as electron-withdrawing groups and electron-donating ones. The inhibition rate

dx.doi.org/10.1021/jm401117t | J. Med. Chem. 2014, 57, 600−612

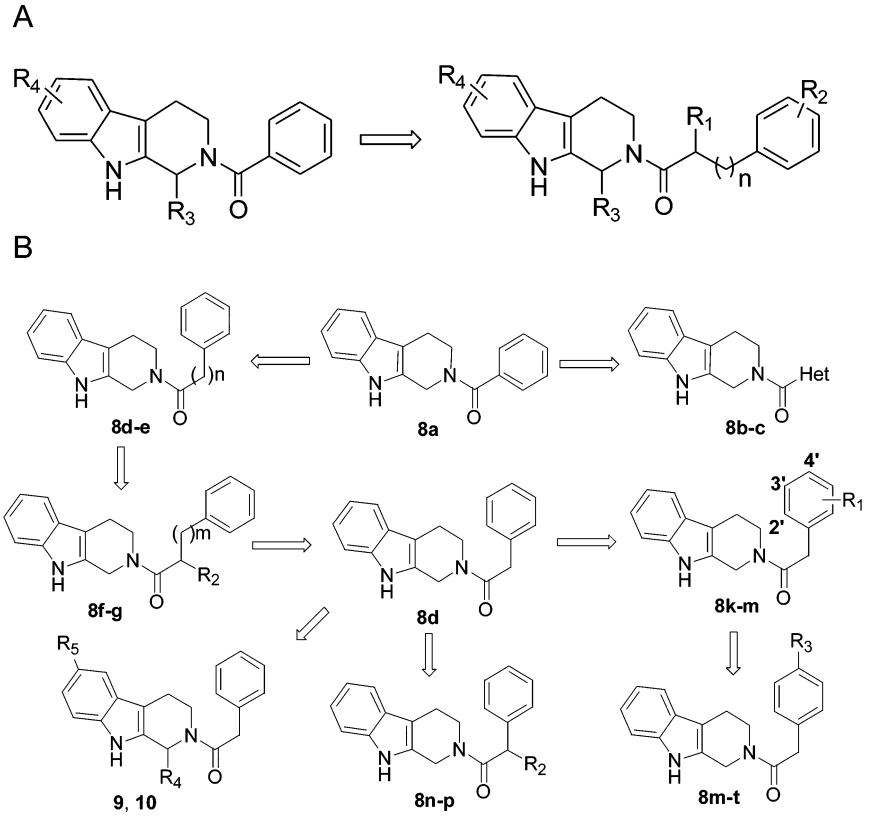

Figure 2. Rational drug design and optimization direction based on initial tetrahydro-β-carboline structure. A, Overall strategies of modifying the initial hit compound. B, The process of optimization of tetrahydro-β-carboline derivatives according to SAR analysis.

Table 2. Effect of Linker Substitutents (R_2) on SBE Luciferase Reporter Gene Expression Inhibition and PC-9 Cell Proliferation

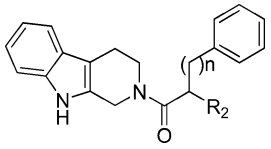

compd. no.	n	R_2	% SBE luciferase inhibition rate (1.0 μM)	% PC-9 cell proliferation inhibition rate (10.0 μM)
8f	0	NHBoc	58.8 ± 5.9	31
8g	1	NHBoc	44.3 ± 1.9	0
8h	0	OH	12.9 ± 0.1	28
8i	0	NH_2	10.9 ± 2.1	11
8j	0	OH, Ph	12.3 ± 0.4	0

Table 3. Effect of Terminal Phenyl Group Substitutions against SBE Luciferase Reporter Gene Expression Inhibition and PC-9 Cell Proliferation

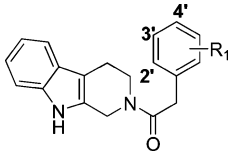

compd. no.	R_1	% SBE luciferase inhibition rate (1.0 μM)	% PC-9 cell proliferation inhibition rate (10.0 μM)
8k	2′-OH	19.7 ± 1.7	33
8l	3′-OH	29.1 ± 3.1	11
8m	4′-OH	64.2 ± 5.9	39
8n	3′-OH,4′-OH	21.0 ± 2.0	26
8o	4′-F	11.8 ± 1.3	21
8p	4′-Cl	7.9 ± 0.4	33
8q	4′-CHO	11.8 ± 1.1	21
8r	4-CH_2Br	50.1 ± 5.3	26
8s	4′-NH_2	18.1 ± 2.1	8
8t	4′-NEt_2	49.0 ± 4.1	18

of compounds with F, Cl, and formyl group (CHO) substitution were 11.8%, 7.9%, and 11.8%, respectively. However, the inhibition rate of those with CH_2Br, NH_2, and NEt_2 were 50.1%, 18.1%, and 49.0%, respectively, which indicated that electron-donating groups were superior to weakly electron-withdrawing groups against SBE luciferase activity. In addition, given the decrease in antiproliferation efficacy of these compounds against PC-9 cells, substitution at this position seemed unsuitable for further optimization, and thus our interest subsequently focused on the optimization of the tetrahydro-β-carboline scaffold other than through 2-position substitution. The 1- and 6-positions were selected for subsequent exploration due to their synthetic convenience. With regard to 1-position substitution, the results clearly revealed that a small aliphatic group substituent was better tolerated than aromatic group substitutions (**9a** vs **9b**). However, the carboxylic acid derivative (**9d**) showed lower activity than compound **9c**. The modifications at the 1-position suggested that R_4 substitution was inclined to small aliphatic group substitutions rather than big aromatic group substitutions, which is consistent with the docking results showing that just a small hydrophobic pocket existed near this position (Figure 3, Table 4).

Finally, the 6-position of tetrahydro-β-carboline was investigated. Three compounds were prepared to explore the

dx.doi.org/10.1021/jm401117t | J. Med. Chem. 2014, 57, 600−612

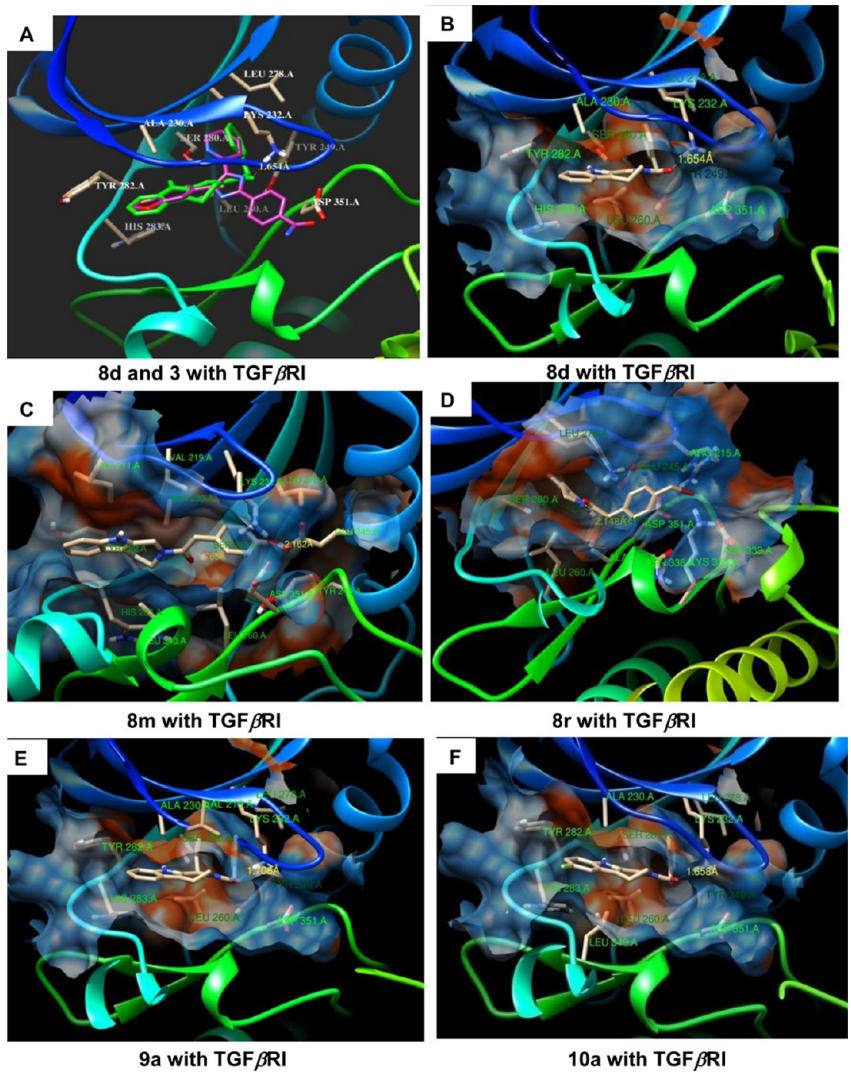

Figure 3. Predictive binding mode of **8d** and **3** (A, **8d** is colored with green, **3** is colored with pink), **8d** (B), **8m** (C), **8r** (D), **9a** (E), and **10m** (F) with the ATP binding site of the TGFβRI kinase domain. β-Carboline warhead of compounds **8d**, **8m**, **9a**, and **10a** bound to the residues His-283 and Tyr-282 in the ATP binding pocket.

Table 4. Effect of 1- or 6-Position Substitution against SBE Reporter Gene Inhibition and PC-9 Cell Proliferation

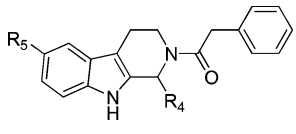

compd. no.	R_4	R_5	% SBE luciferase inhibition rate (1.0 μM)	% PC-9 cell proliferation inhibition rate (10.0 μM)
9a	Et	H	52.1 ± 4.9	24
9b	Ph	H	10.3 ± 1.0	10
9c	CH_2CO_2Me	H	18.2 ± 1.7	ND[a]
9d	CH_2CO_2H	H	4.1 ± 0.2	9
10a	H	F	ND	78
10b	H	Br	ND	47
10c	CH_3	OH	11.2 ± 1.2	8

[a]ND: not detected.

feasibility of increasing antitumor efficacy by varying this position. Among the compounds modified in this position, compound **10a** was nearly as good as compound **8d** in inhibiting PC-9 cell line proliferation (Table 5). Therefore, a halogen substituent, especially a fluoro group, might reveal more activity than a hydroxyl group in this position.

Table 5. Antiproliferative Activity of Compounds 8d and 10a in Three Different Lung Cancer Cell Lines

	IC_{50} (μM)		
compd. no.	PC-9	H1299	A549
8d	5.87	8.07	7.90
10a	7.09	6.19	4.85

To further evaluate the antiproliferative properties of this series of compounds against different lung cancer cell lines, compounds **8d** and **10a** were chosen for testing their IC_{50} values based on their inhibition rate against PC-9 cells. Both of these two compounds showed antiproliferative activities against three different lung cancer cell lines (PC-9, H1299, and A549 cell lines, Table 5). These results supported that these compounds showed inhibitory activities in vitro cell based assays.

To account for how these potent compounds interacted with TGFβRI, we used the TGFβRI (PDB ID: 3TZM) docking model both unbound and in complex with compound **3** as

dx.doi.org/10.1021/jm401117t | J. Med. Chem. 2014, 57, 600−612

described in our previous publication to analyze the binding mode of different compounds with compound **3** as a positive control.[26] As shown in Figure 3A, the interaction mode was also similar to **3** (pink), with the β-carboline warhead of compound **8d** (green) binding to the "goal keeper" residues His-283 and Tyr-282 in the ATP binding pocket, as reported elsewhere for other compounds.[25] N−H and carbonyl groups of compound **8d** (gray) were bound to residues Tyr249 and Lys232, respectively, in the ATP binding pocket by hydrogen bonds, and the benzyl moiety interacted with the hydrophobic area which was formed by the residues Lys232, Tyr249, and Leu278 (Figure 3B). Analysis of the docking experiments for compounds **8m** (Figure 3C) showed that two hydrogen bonds were formed: carbonyl to Ser280, and hydroxyl to Glu245. On the other hand, the docking model of compound **8r** (Figure 3D) showed that, although the binding model was changed, a hydrogen bond was still formed between N−H and the hydroxyl group of Tyr249 to keep the bioactivity. For compound **9a** (Figure 3E), introducing an ethyl group at the 1-position of carboline seemed to make no difference to the

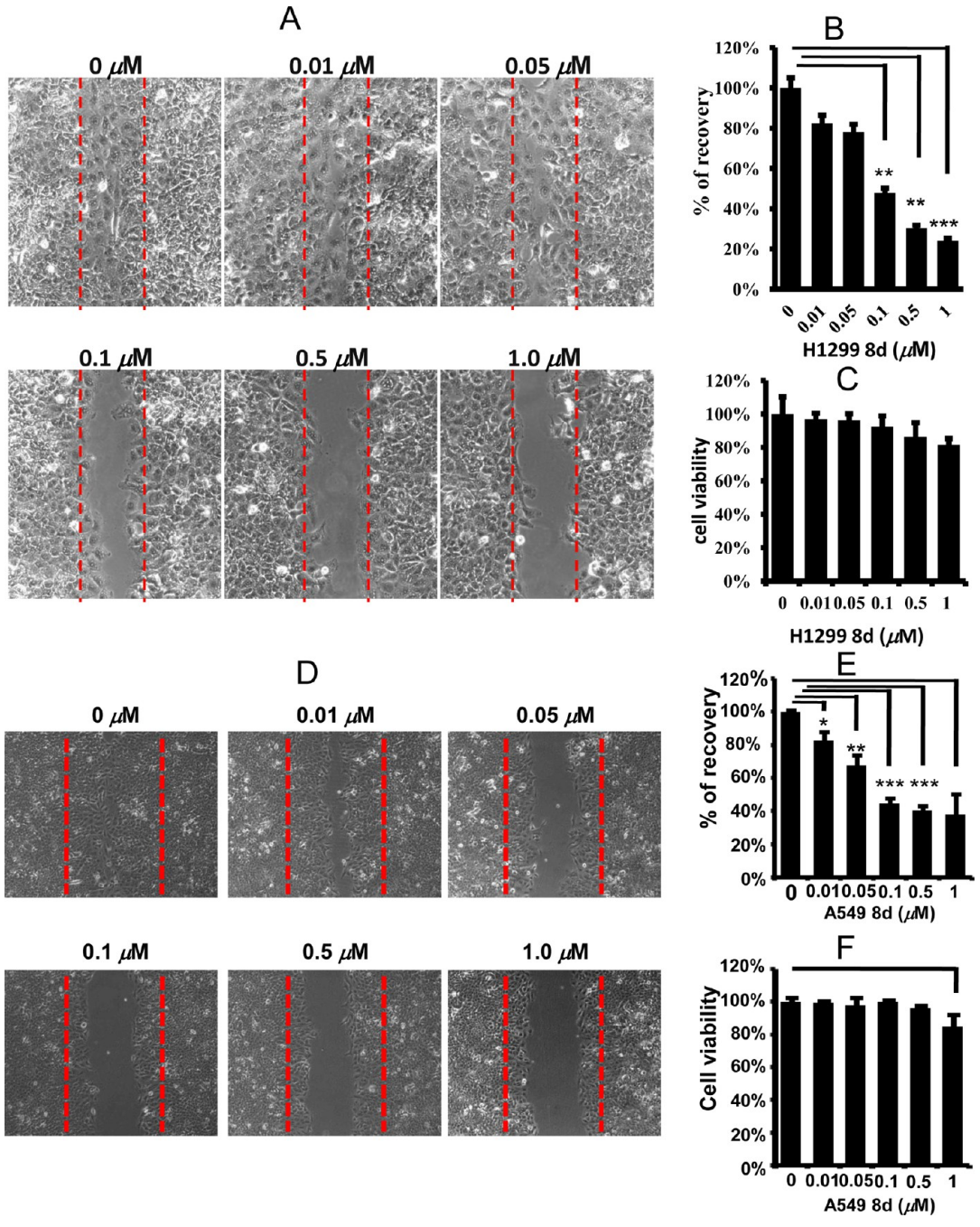

Figure 4. Compound **8d** inhibits migration of lung cancer H1299 and A549 in a wound healing assay. (A, B) A wound was made on a confluent plate of H1299 cells treated as indicated. The effect of indicated concentrations of **8d** against lung cancer H1299 cell migration into the wound was determined after 12 h. (C) The effect of compound **8d** on H1299 cell viability after 12 h treatment. (D, E) The effect of **8d** against A549 lung cancer cell migration. (F) The effect of compound **8d** on A549 cell viability after 12 h treatment. Values are means ± SD, ** indicates $p < 0.01$, *** indicates $p < 0.001$ as determined by Student's t test.

dx.doi.org/10.1021/jm401117t | J. Med. Chem. 2014, 57, 600−612

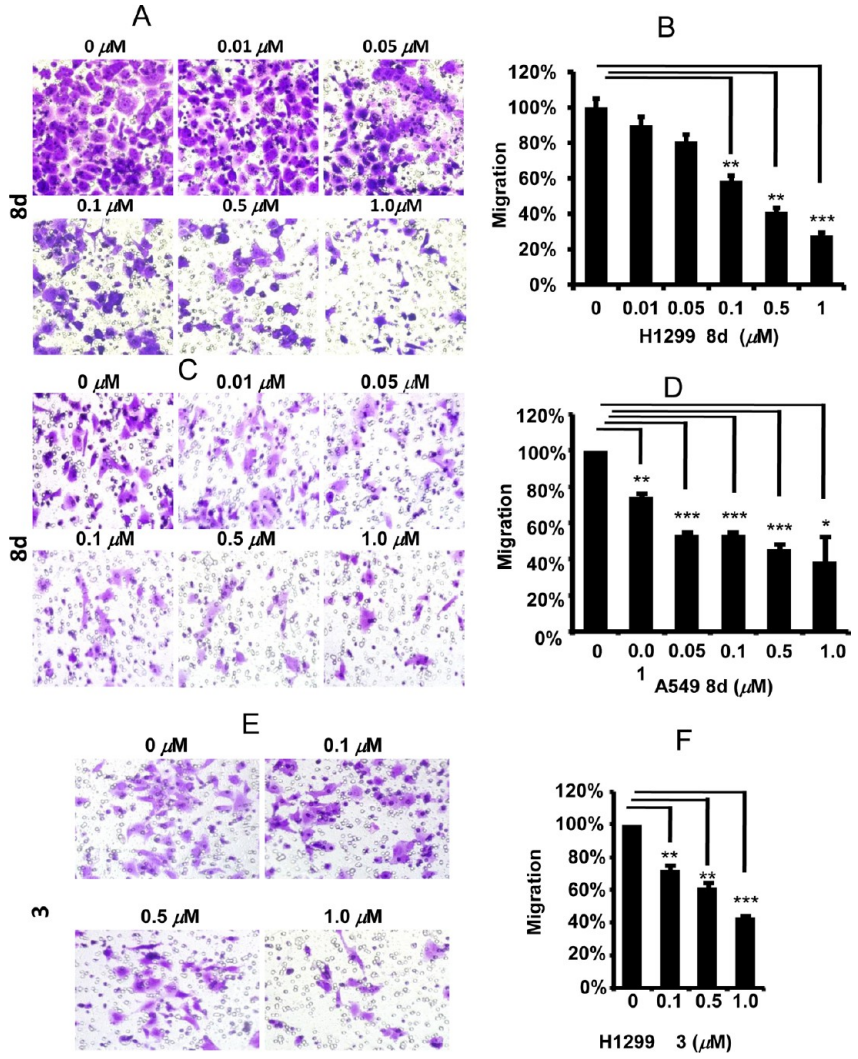

Figure 5. Compound **8d** inhibits transwell migration of H1299 and A549 lung cancer cells. (A, B) H1299 cells were plated in the top chamber of a transwell insert and assayed for transwell migration while treated with indicated concentrations of **8d**. (C, D) Effect of indicated concentrations of **8d** on A549 lung cancer cell transwell migration. (E, F) Transwell migration inhibitory effect of indicated concentrations of **3** on lung cancer H1299 cells, performed as a positive control. Values are means ± SD, ** indicates $p < 0.01$, *** indicates $p < 0.001$ as determined by Student's t test.

binding mode but resulted in lower inhibitory activity. For compound **10a**, a fluorine at the 6-position of carboline made little difference compared with **8d**, as hydrogen bonds were also present between the carboline N−H group and Ser280, and the carbonyl group and Lys232 (Figure 3F).

Tumor cell migration and invasion are critical parameters of cancer metastasis, which is the most common cause of death in cancer patients.[31] To investigate the antimigratory effect of this series of compounds against a lung cancer cell line, compound **8d** was selected based on its high signaling pathway inhibition and anticancer cell proliferation efficacy for evaluation using the wound-healing model as well as transwell migration assays in H1299 cells and A549 cells. As shown in Figure 4A and 4D, compound **8d** decreased H1299 and A549 cell migration in a dose-dependent manner in the wound-healing model, with the IC_{50} approximately 0.1 μM (Figure 4B and 4E). The antiproliferation efficacy of this compound was also determined at the same time; compound **8d** had little effect against cell viability even at 1.0 μM concentration for 12 h (Figure 4C and 4F), suggesting that the compound mainly inhibited cell migration rather than proliferation. In another migration model, compound **8d** also revealed similarly potent inhibition against H1299 cell and A549 cell migration with an IC_{50} less than 0.5 μM (Figure 5A−D), compared to a similar inhibition of compound **3** as positive control which had an IC_{50} about 0.5−1.0 μM in the same H1299 cell invasion model (Figure 5E and 5F). Both of these data demonstrated that this compound strongly inhibited lung cancer cell migration at submicromolar concentration. We also found consistent results that compound **8d** inhibited cell migration in different breast cancer cell lines.[26]

Cell motility is responsible for cell migration and invasion, and growing evidence implies that inhibition of tumor cell motility would limit cell migration and invasion.[32] This suggests that targeting tumor cell motility is also a valuable strategy for the inhibition of tumor metastasis.[33] To further investigate the influence of this series of compounds against lung cancer cell motility, another experiment using the live-cell tracking assay was performed. As shown in Figure 6A and 6B, eight random cells per condition were selected for observation in the microscope field of vision. In the absence of compound **8d**, cells moved chaotically (Figure 6A). However, those cells treated with compound **8d** were found to track a much shorter distance, and cell velocities were also reduced with treatment of **8d** compared with the control group. These observations

dx.doi.org/10.1021/jm401117t | J. Med. Chem. 2014, 57, 600−612

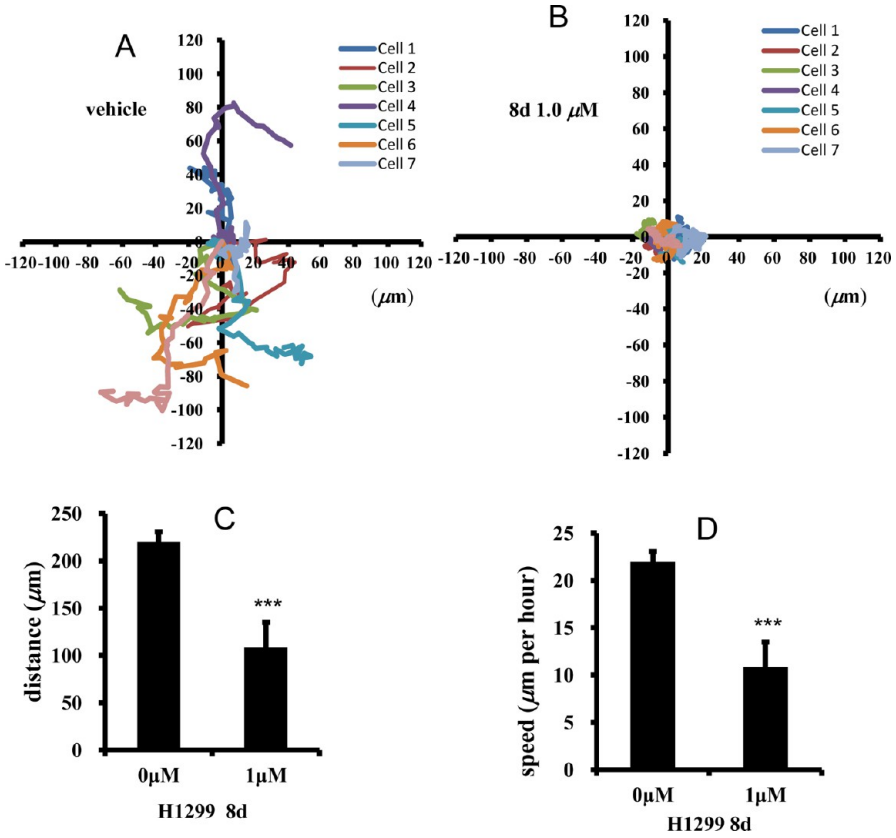

Figure 6. Live-cell tracking assay reveals that **8d** reduces motility in lung cancer cells. H1299 cells incubated with or without **8d** were observed by time-lapse video microscopy. The movement track of each individual cell was analyzed by Image-pro plus 6.0. The distance (H) and speed (I) of migration were extracted from the track-plots. The different colors represent different cells analyzed. Values are mean ± SD, ** indicates $p < 0.01$, *** indicates $p < 0.001$ as determined by Student's t test.

suggested that compound **8d** repressed tumor cell motility with high potency.

To evaluate the effect of this compound against tumor growth in vivo, we performed xenograft human lung cancer cell mouse model tumor formation experiments. We selected gefitinib, a broadly used therapeutic against nonsmall-cell lung carcinoma (NSCLC), as a positive control. Our results demonstrated that compound **8d** significantly suppressed the tumor volume with a dose of 5.0 mg/kg/day (ip), which was superior to the effect of gefitinib at a dose of 20 mg/kg/day (ip) (Figure.7A), and both of these compounds had little effect on mouse body weight (Figure 7B). Taken together, these data indicated that compound **8d** could repress lung cancer growth in vivo.

To further evaluate the inhibitory effect of compound **8d** on the growth of other tumor in vivo, we performed additional tumor growth assays using an orthotopic model. We injected mouse breast cancer 4T1-luciferase cells into Balb/c mouse mammary glands and treated the mice with compound **8d** at either 1.0 mg/kg/day or 5.0 mg/kg/day. After 20 days, we analyzed orthotopic breast cancer cell bioluminescene to evaluate the tumor growth. Our data indicated that compound **8d** also suppressed primary breast cancer growth in a dose-dependent manner (Figure 7C and 7D).

■ CONCLUSION

Beginning with a virtual screen against the TGFβRI kinase domain, we identified a series of tetrahydro-β-carboline derivatives as a novel class of inhibitors of the TGFβ signaling pathway. Optimization based on the initial hit contributed to the discovery of phenylacetyl tetrahydro-β-carbolines as potent inhibitors of the TGFβ signaling pathway. These compounds not only inhibited cancer cell proliferation but also inhibited cancer cell migration in the wound-healing and transwell assays. Furthermore, some compounds also obviously inhibited tumor cell motility compared with the control group. Compound **8d** significantly inhibited lung cancer and breast cancer growth in vivo at the dose of 5.0 mg/kg/day (ip) as expected. These data combined with our preliminary results revealed that compound **8d** might be a potential anticancer agent against lung cancer and breast cancer.

■ EXPERIMENTAL SECTION

General Methods for Chemistry. All starting materials were commercially available and used without further purification. All reactions were carried out with the use of standard techniques under an inert atmosphere (Ar or N_2). NMR spectra were generated on a Bruker 300 or 400 MHz instrument and obtained as $CDCl_3$ or DMSO-d_6 solutions (reported in ppm), using $CDCl_3$ as the reference standard (7.26 ppm) or DMSO-d_6 (2.50 ppm). Mass spectral data (ESI) were gathered on VG ZAB-HS or VG-7070 instrument. HPLC (Agilent Technologies 1200 Series) was employed for purity determination, using the following method: Eclipse XDB C18 column, 5 μm, 4.6 mm × 150 mm, column temperature 40 °C; solvent A: water; solvent B: MeOH; gradient of 40−70% B (0−10 min), 70−90% B (10 −15 min), 90−40% B (15−20 min); flow rate of 1.5 mL/min. Compound purity was determined by high pressure liquid chromatography (HPLC) with a confirming purity of ≥95% for all of the final biologically tested compounds.

dx.doi.org/10.1021/jm401117t | J. Med. Chem. 2014, 57, 600−612

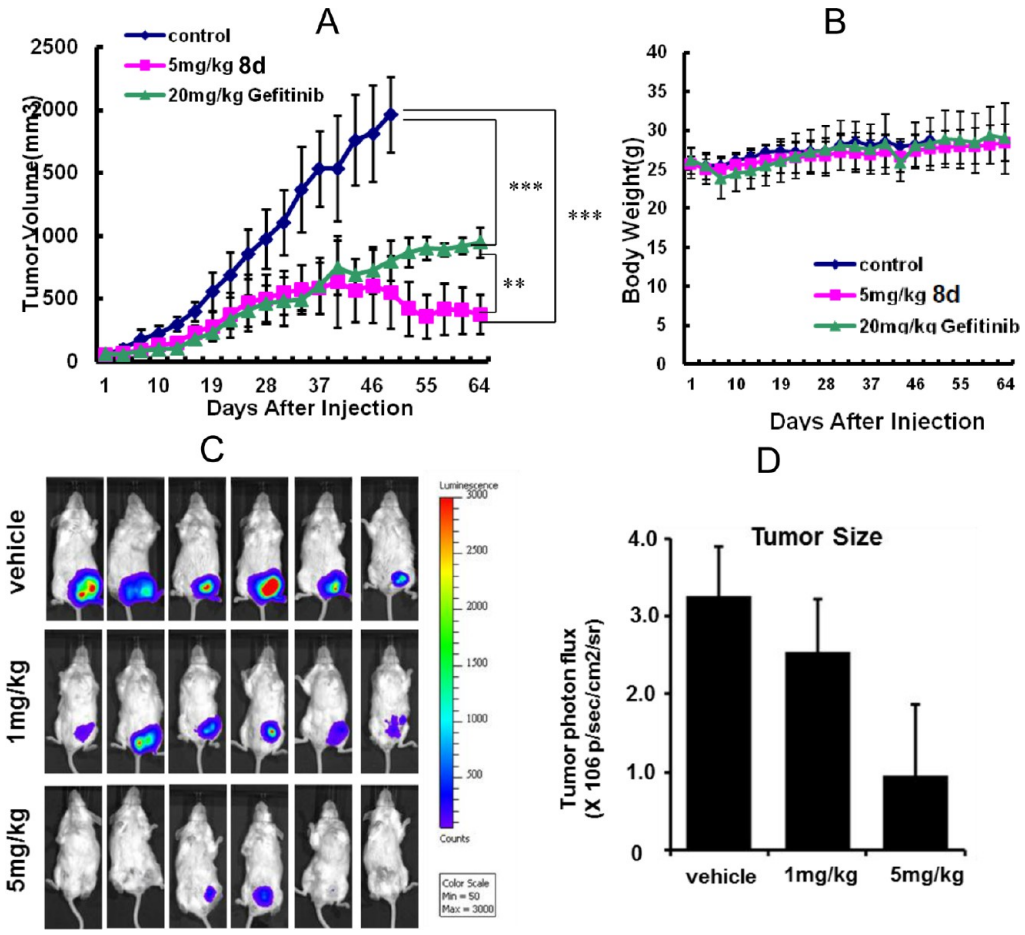

Figure 7. Compound **8d** inhibits lung and breast cancer cell growth in vivo. (A, B) Mice subcutaneously injected with A549 cells were treated were treated as indicated and effects on tumor volumes (A) and body weight (B) were measured. (C, D) Mice were orthotopically injected with 4T1-luc cells and treated as indicated for 20 days. Tumor cells were detected by in vivo imaging (C), and bioluminescence intensity was quantitated (D). Graph shows mean ± SD, *** $P < 0.001$.

***N*-Benzoyl-1,3,4,9-tetrahydro-β-carboline (8a).** To a solution of benzoic acid (122 mg, 1.0 mmol) in anhydrous DMF (5 mL) were added EDC (249 mg, 1.3 mmol) and HOBt (149 mg, 1.1 mmol) at 0 °C, and then 1,3,4,9-tetrahydro-β-carboline (172 mg, 1.0 mmol) was added to the mixture after stirring for 15 min. The mixture was stirred for another 3 h, diluted with H_2O, and extracted with EtOAc (3 × 60 mL). The combined organic phase was dried over anhydrous Na_2SO_4, concentrated, and chromatographed over silica gel to give 177 mg (64% yield) of compound **8a**. ^{1}H NMR (300 MHz, $CDCl_3$): δ 7.47 (br s, 1H), 7.49−7.45 (m, 6H), 7.34−7.31 (m, 1H), 7.16−7.09 (m, 2H), 4.99−4.92 (m, 2H), 3.79−3.70 (m, 2H), 2.88−2.83 (m, 2H). MS (ESI): *m*/*z*: 275 $[M - H]^-$.

***N*-(2-Thiophenecarbonyl)-1,3,4,9-tetrahydro-β-carboline (8b).** The title compound was synthesized according to the procedure of preparing **8a** except using 2-thenoic acid instead of benzoic acid. Yield: 70%. ^{1}H NMR (DMSO, 400 MHz): δ 10.86 (br s, 1H), 7.79 (d, *J* = 5.0 Hz, 1H), 7.53 (d, *J* = 0.2 Hz, 1H), 7.41 (d, *J* = 7.7 Hz, 1H), 7.31 (d, *J* = 7.9 Hz, 1H), 7.17 (dd, *J* = 4.4, 4.2 Hz, 1H), 7.04 (dd, *J* = 7.7, 7.2 Hz, 1H), 6.97 (dd, *J* = 7.4, 7.3 Hz, 1H), 4.86−4.82 (m, 2H), 3.95 (dd, *J* = 5.6, 5.5 Hz, 2H), 2.86−2.80 (m, 2H); MS (ESI): *m*/*z*: 281 $[M - H]^-$.

***N*-(2-Pyridinylcarbonyl)-1,3,4,9-tetrahydro-β-carboline (8c).** The title compound was synthesized according to the procedure of preparing **8a** except using 2-pyridinecarboxylic acid instead of benzoic acid. Yield: 68%. ^{1}H NMR ($CDCl_3$, 400 MHz): δ 10.63 (br s, 1H), 8.41−8.37 (m, 1H), 7.67−7.63 (m, 1H), 7.35 (d, J = 7.6 Hz, 1H), 7.22−7.13 (m, 3H), 6.84−6.80 (m, 2H), 4.72 (br s, 2H), 3.31−3.20 (m, 2H), 2.55−2.54 (m, 2H); MS (ESI): *m*/*z*: 281 $[M - H]^-$.

***N*-Phenylacetyl-1,3,4,9-tetrahydro-β-carboline (8d).** The title compound was synthesized according to the procedure of preparing **8a** except using phenylacetic acid instead of benzoic acid. Yield: 70%. ^{1}H NMR (DMSO, 400 MHz): δ 10.83 (br s, 1H), 7.39−7.28 (m, 6H), 7.22−7.20 (m, 1H), 7.03−7.00 (m, 1H), 6.95−6.91 (m, 1H), 4.72−4.66 (m, 2H), 3.88−3.86 (m, 2H), 3.83−3.80 (m, 2H), 2.61−2.55 (m, 2H); MS (ESI): *m*/*z*: 313 $[M + Na]^+$.

***N*-(3-Phenylpropanoyl)-1,3,4,9-tetrahydro-β-carboline (8e).** The title compound was synthesized according to the procedure of preparing **8a** except using 3-phenylpropanoic acid instead of benzoic acid. Yield: 80%. ^{1}H NMR (DMSO, 400 MHz): δ 10.79 (br s, 1H), 7.39−7.35 (m, 1H), 7.30−7.24 (m, 5H), 7.18−7.14 (m, 1H), 7.02 (dd, *J* = 7.7, 7.2 Hz, 1H), 6.94 (dd, *J* = 7.5, 7.3 Hz, 1H), 4.68−4.62 (m, 2H), 3.82−3.73 (m, 2H), 2.87−2.80 (m, 2H), 2.77−2.65 (m, 4H); MS (ESI): *m*/*z*: 327 $[M + Na]^+$.

***N*-(2-(*tert*-Butoxycarbonylamino)phenylacetyl)-1,3,4,9-tetrahydro-β-carboline (8f).** The title compound was synthesized according to the procedure of preparing **8a** except using 2-(*tert*-butoxycarbonylamino)phenylacetic acid instead of benzoic acid. Yield: 54%. ^{1}H NMR (400 MHz, DMSO): δ 10.83 (br s, 1H), 7.41 (d, *J* = 7.2 Hz, 2H), 7.36 (d, *J* = 7.2 Hz, 2H), 7.32−7.31 (m, 2H), 7.29−7.28 (m, 2H), 7.00 (dd, *J* = 8.0, 7.6 Hz, 1H), 6.92 (dd, *J* = 8.0, 7.6 Hz, 1H), 6.93−6.90 (m, 1H), 5.72 (d, *J* = 8.0 Hz, 1H), 4.77 (d, *J* = 16.8 Hz, 1H), 4.65 (d, *J* = 16.8 Hz, 1H), 3.81−3.76 (m, 1H), 3.73−3.68 (m, 1H), 2.67−2.63 (m, 1H), 2.11−2.09 (m, 1H), 1.37 (s, 9H); MS (ESI): *m*/*z*: 428 $[M + Na]^+$.

***N*-(2-(*tert*-Butoxycarbonylamino)-3-phenylpropanoyl)-1,3,4,9-tetrahydro-β-carboline (8g).** The title compound was synthesized according to the procedure of preparing **8a** except using

dx.doi.org/10.1021/jm401117t | *J. Med. Chem.* 2014, 57, 600−612

2-(*tert*-butoxycarbonylamino)-3-phenylpropanoic acid instead of benzoic acid. Yield: 54%. ^{1}H NMR ($CDCl_3$, 400 MHz): δ 10.83 (br s, 1H), 7.37−7.35 (m, 1H), 7.30−7.28 (m, 2H), 7.26−7.24 (m, 2H), 7.21−7.18 (m, 2H), 7.03 (dd, J = 7.2, 7.2 Hz, 1H), 6.95 (dd, J = 7.2, 7.2 Hz, 1H), 4.82−4.72 (m, 2H), 4.54−4.50 (m, 1H), 3.88−3.84 (m, 2H), 2.69−2.61 (m, 2H), 2.45−2.41 (m, 2H), 1.30 (s, 9H); MS (ESI): m/z: 454 $[M + Cl]^-$.

***N*-(2-Hydroxy-2-phenylacetyl)-1,3,4,9-tetrahydro-β-carboline (8h).** The title compound was synthesized according to the procedure of preparing **8a** except using 2-hydroxy-2-phenylacetic acid instead of benzoic acid. Yield: 22%. ^{1}H NMR ($CDCl_3$, 400 MHz): δ 10.86 (br s, 1H), 7.42−7.36 (m, 4H), 7.34−7.31 (m, 3H), 7.15 (dd, J = 8.4, 8.4 Hz, 1H), 6.92 (dd, J = 8.4, 8.4 Hz, 1H), 5.83−5.73 (m, 2H), 5.49 (d, J = 10.0 Hz, 1H), 4.81−4.73 (m, 2H), 3.84−3.78 (m, 2H); MS (ESI): m/z: 329 $[M + Na]^+$.

***N*-(2-Amino-2-phenylacetyl)-1,3,4,9-tetrahydro-β-carboline (8i).** To a solution of **8f** (245 mg, 0.6 mmol) in DCM (10 mL) was injected TFA (0.5 mL) at 0 °C, and then the reaction was stirred at room temperature for 3 h. The solvent was evaporated under reduced pressure, and the pH value was adjusted to pH = 12 with 10% NaOH solution. Then the solution was extracted with EtOAc, washed with saturated brine, and dried over anhydrous Na_2SO_4. The crude product was purified by gel column chromatography (eluent, $CHCl_3$:MeOH = 100:1 to 20:1) to give compound **8i** (83 mg, 45%). ^{1}H NMR (400 MHz, DMSO): δ 10.84 (br s, 1H), 7.41−7.39 (m, 2H), 7.36−7.33 (m, 2H), 7.30−7.25 (m, 3H), 7.02 (dd, J = 7.2, 7.2 Hz, 1H), 6.96−6.90 (m, 1H), 5.07−5.01 (m, 1H), 4.82−4.65 (m, 2H), 3.82−3.66 (m, 2H), 2.68−2.58 (m, 1H), 2.16−2.09 (m, 1H); MS (ESI): m/z: 306 $[M + H]^+$.

***N*-(2-Hydroxy-2-phenyl-2-phenylacetyl)-1,3,4,9-tetrahydro-β-carboline (8j).** The title compound was synthesized according to the procedure of preparing **8a** except using 2-hydroxy-2,2-diphenylacetic acid instead of benzoic acid. Yield: 23%. ^{1}H NMR ($CDCl_3$, 400 MHz): δ 8.01 (br s, 1H), 7.44−7.39 (m, 3H), 7.37−7.34 (m, 2H),7.31−7.27 (m, 4H), 7.26−7.24 (m, 2H), 7.14 (dd, J = 7.6, 7.6 Hz, 2H), 7.07−7.05 (m, 1H), 5.00 (br s, 2H), 3.52 (br s, 2H), 2.95−2.88 (m, 2H); MS (ESI): m/z: 405 $[M + Na]^+$.

***N*-(2-Hydroxyphenylacetyl)-1,3,4,9-tetrahydro-β-carboline (8k).** The title compound was synthesized according to the procedure of preparing **8a** except using 2-hydroxyphenylacetic acid instead of benzoic acid. Yield: 82%. ^{1}H NMR (300 MHz, DMSO): δ 10.10 (br s, 1H), 9.57 (s, 1H), 7.40−7.28 (m, 2H), 7.08−6.80 (m, 4H), 6.82−6.69 (m, 2H), 4.70 (s, 2H), 3.86−3.80 (m, 2H), 3.72 (s, 2H), 2.64−2.60 (m, 2H); MS (ESI): m/z: 329 $[M + Na]^+$.

***N*-(3-Hydroxyphenylacetyl)-1,3,4,9-tetrahydro-β-carboline (8l).** The title compound was synthesized according to the procedure of preparing **8a** except using 3-hydroxyphenylacetic acid instead of benzoic acid. Yield: 30%. ^{1}H NMR (300 MHz, DMSO): δ 10.83 (br s, 1H), 9.29 (br s, 1H), 7.38−7.32 (m, 1H), 7.27 (d, J = 8.0 Hz, 1H), 7.11−6.89 (m, 3H), 6.69−6.67 (m, 2H), 6.64−6.59 (m, 1H), 4.68 (s, 2H), 3.84−3.72 (m, 4H), 2.68−2.48 (m, 2H); MS (ESI): m/z: 329 $[M + Na]^+$.

***N*-(4-Hydroxyphenylacetyl)-1,3,4,9-tetrahydro-β-carboline (8m).** The title compound was synthesized according to the procedure of preparing **8a** except using 4-hydroxyphenylacetic acid instead of benzoic acid. Yield: 65%. ^{1}H NMR (DMSO, 400 MHz): δ 10.93 (br s, 1H), 9.35 (br s, 1H), 7.38−7.29 (m, 2H), 7.30−7.24 (m, 5H), 7.10−6.99 (m, 4H), 6.74−6.67 (m, 2H), 4.74−4.68 (m, 2H), 3.86−3.83 (m, 2H), 3.81−3.79 (m, 2H), 2.60−2.56 (m, 2H); MS (ESI): m/z: 305 $[M - H]^-$.

***N*-(3,4-Dihydroxyphenylacetyl)-1,3,4,9-tetrahydro-β-carboline (8n).** The title compound was synthesized according to the procedure of preparing **8a** except using 3,4-dihydroxyphenylacetic acid instead of benzoic acid. Yield: 31%. ^{1}H NMR (DMSO, 400 MHz): δ 10.82 (br s, 1H), 8.83 (br s, 1H), 8.72 (br s, 1H), 7.35 (d, J = 8.0 Hz, 1H), 7.27 (d, J = 8.0 Hz, 1H), 7.01 (dd, J = 8.0, 8.0 Hz, 1H), 6.94−6.91 (m, 1H), 6.66−6.62 (m, 2H), 6.53−6.47 (m, 1H), 4.66 (br s, 2H), 3.74−3.71 (m, 2H), 3.64−3.61 (m, 2H), 2.66−2.64 (m, 2H); MS (ESI): m/z: 345 $[M + Na]^+$.

***N*-(4-Fluorophenylacetyl)-1,3,4,9-tetrahydro-β-carboline (8o).** The title compound was synthesized according to the procedure of preparing **8a** except using 4-fluorophenylacetic acid instead of benzoic acid. Yield: 57%. ^{1}H NMR (300 MHz, DMSO): δ 10.82 (br s, 1H), 7.40−7.34 (m, 1H), 7.32−7.27 (m, 3H), 7.15−7.09 (m, 2H), 7.03 (dd, J = 7.8, 7.2 Hz, 1H), 6.94 (dd, J = 7.8, 7.2 Hz, 1H), 4.72−4.69 (m, 2H), 3.86−3.84 (m, 2H), 3.83−3.81 (m, 2H), 2.67−2.62 (m, 1H); MS (ESI): m/z: 331 $[M + Na]^+$.

***N*-(4-Chlorophenylacetyl)-1,3,4,9-tetrahydro-β-carboline (8p).** The title compound was synthesized according to the procedure of preparing **8a** except using 4-chlorophenylacetic acid instead of benzoic acid. Yield: 52%. ^{1}H NMR (DMSO, 300 MHz): δ 10.83 (br s, 1H), 7.36−7.31 (m, 3H), 7.29−7.21 (m, 3H), 7.01 (dd, J = 7.2, 7.2 Hz, 1H), 6.92 (dd, J = 7.2, 7.2 Hz, 1H), 4.68 (br s, 2H), 3.85−3.80 (m, 4H), 2.64−2.61 (m, 2H); MS (ESI): m/z: 347 $[M + Na]^+$.

***N*-(4-Formylphenylacetyl)-1,3,4,9-tetrahydro-β-carboline (8q).** The title compound was synthesized according to the procedure of preparing **8a** except using 4-formylphenylacetic acid instead of benzoic acid. Yield: 35%. ^{1}H NMR (300 MHz, DMSO): δ 10.88 (br s, 1H), 9.97 (s, 1H), 7.87−7.83 (m, 2H), 7.52−7.44 (m, 2H), 7.41−7.36 (m, 1H), 7.31−7.28 (m, 1H), 7.06−7.01 (m, 1H), 6.98−6.93 (m, 1H), 4.71 (s, 2H), 4.00 (s, 2H), 3.85 (t, J = 5.4 Hz, 2H), 2.67 (t, J = 5.4 Hz, 2H); MS (ESI): m/z: 353 $[M + Cl]^-$.

***N*-(4-Bromomethylphenylacetyl)-1,3,4,9-tetrahydro-β-carboline (8r).** The title compound was synthesized according to the procedure of preparing **8a** except using 4-bromomethylphenylacetic acid instead of benzoic acid. Yield: 45%. ^{1}H NMR ($CDCl_3$, 300 MHz): δ 8.21 (br s, 1H), 7.55−7.46 (m, 2H), 7.42−7.37 (m, 4H), 7.29−7.20 (m, 2H), 4.96 (s, 2H), 4.69 (s, 2H), 4.00−3.88 (m, 4H), 2.88−2.79 (m, 2H).

***N*-(4-Aminophenylacetyl)-1,3,4,9-tetrahydro-β-carboline (8s).** A solution of *N*-(4-nitrophenylacetyl)-1,3,4,9-tetrahydro-β-carboline (336 mg, 1.0 mmol), iron powder (5.0 mmol), and NH_4Cl (106 mg, 2.0 mmol) in EtOH/H_2O (12 mL/3 mL) was heated to reflux for 2 h. The solvent was concentrated under reduced pressure, and then the crude product was purified by gel column chromatography (PE:EA = 6:1 to 1:1) to give compound **8s** (159 mg, 52%). ^{1}H NMR (300 MHz, DMSO): δ 10.83 (br s, 1H), 9.29 (br s, 1H), 7.38−7.32 (m, 1H), 7.27 (d, J = 8.0 Hz, 1H), 7.11−6.89 (m, 3H), 6.69−6.67 (m, 2H), 6.64−6.59 (m, 1H), 4.68 (s, 2H), 3.84−3.72 (m, 4H), 2.68−2.48 (m, 2H); MS (ESI): m/z: 328 $[M + Na]^+$.

***N*-(4-Diethylaminophenylacetyl)-1,3,4,9-tetrahydro-β-carboline (8t).** To a solution of **8s** (306 mg, 1.0 mmol) and K_2CO_3 (695 mg, 5 mmol) in DMF (5 mL) was injected 2-bromoethane (300 μL, 4.0 mmol) under ice cooling, and then the reaction mixture and stirred for 6 h at rt. The reaction mixture was extracted with EtOAc, washed with brine, and dried over anhydrous Na_2SO_4. The solvent was concentrated under reduced pressure, and then the crude product was purified by gel column chromatography (PE:EA = 6:1 to 2:1) to give compound **8t** (145 mg, 40%). ^{1}H NMR (DMSO, 300 MHz): δ 10.72 (br s, 1H), 7.17 (dd, J = 7.5, 7.5 Hz, 2H), 6.92−6.88 (m, 2H), 6.85−6.79 (m, 2H), 6.46 (d, J = 8.4 Hz, 2H), 4.55 (br s, 2H), 3.68−3.64 (m, 2H), 3.53−3.51 (m, 2H), 2.50−2.43 (m, 2H), 2.37−2.33 (m, 4H), 0.93 (t, J = 6.9 Hz, 6H).

1-Ethyl-*N*-phenylacetyl-1,3,4,9-tetrahydro-β-carboline (9a). To a solution of tryptamine (320 mg, 2.0 mmol) in 5% TFA/DCM (5 mL) was added propionaldehyde (216 μL, 3.0 mmol), and the mixture was stirred at rt for 8 h. The solvent was concentrated under reduced pressure. The residue was treated with 10% NaOH to pH = 12, extracted with EtOAc, washed with water, and dried over anhydrous Na_2SO_4. The solvent was concentrated in vacuo to afford 1-ethyl-1,3,4,9-tetrahydro-β-carboline (280 mg), which was treated using a method similar to that for **8a** to give **9a** (213 mg, 35%). ^{1}H NMR (300 MHz, $CDCl_3$): δ 8.58 (br s, 1H), 7.53−7.50 (m, 1H), 7.45−7.37 (m, 6H), 7.25 (dd, J = 7.5, 7.5 Hz, 1H), 7.21−7.16 (m, 1H), 5.90 (t, J = 6.9 Hz, 1H), 4.23−4.19 (m, 1H), 4.04−4.00 (m, 2H), 3.60−3.49 (m, 1H), 2.81−2.75 (m, 1H), 2.68−2.58 (m, 1H), 2.09−2.03 (m, 1H), 1.98−1.90 (m, 1H), 1.88−1.86 (m, 2H), 1.13 (t, J = 7.5 Hz, 1H); MS (ESI): m/z: 341 $[M + Na]^+$.

1-Phenyl-*N*-phenylacetyl-1,3,4,9-tetrahydro-β-carboline (9b). The title compound was synthesized according to the procedure of preparing **9a** except using benzaldehyde instead of propionaldehyde.

dx.doi.org/10.1021/jm401117t | J. Med. Chem. 2014, 57, 600−612

Yield: 49%. ^{1}H NMR (300 MHz, $CDCl_3$): δ 8.18 (br s, 1H), 7.46 (d, J = 7.5 Hz, 1H), 7.25−7.16 (m, 11H), 7.13−7.08 (m, 2H), 3.96−3.90 (m, 1H), 3.81−3.74 (m, 2H), 3.38−3.30 (m, 1H), 2.76−2.70 (m, 1H), 2.60−2.56 (m, 1H), 1.71−1.68 (m, 1H). ^{13}C NMR (400 MHz, $CDCl_3$): δ 22.1, 40.5, 41.5, 52.3, 109.7, 111.5, 118.2, 119.6, 122.2, 126.7, 127.0, 128.2, 128.6, 128.8, 128.9, 131.8, 135.1, 136.5, 140.1, 170.0; MS (ESI): m/z: 389 $[M + Na]^+$.

1-Methoxycarbonylmethyl-*N*-phenylacetyl-1,3,4,9-tetrahydro-*β*-carboline (9c). To a solution of tryptamine (320 mg, 2.0 mmol) in acetic acid (8 mL) was slowly added methyl 3,3-dimethoxypropionate (320 μL, 2.2 mmol), and the mixture was heated to reflux for 4 h. The solvent was removed in vacuo, and then the residue was treated with 10% NaOH to pH = 12, extracted with EtOAc, washed with water, and dried over anhydrous Na_2SO_4. The solvent was concentrated in vacuo to afford 1-methoxycarbonylmethyl-1,3,4,9-tetrahydro-*β*-carboline (280 mg, 1.1 mmol), which was treated with a method similar to that for **8a** to give **9c**, which was purified by gel column chromatography (eluent, PE:EA = 6:1 to 1:1) to give **9c** as a white solid. Yield 68%. ^{1}H NMR (300 MHz, $CDCl_3$): δ 8.91 (br s, 1H), 7.32 (d, J = 7.8 Hz, 1H), 7.34−7.31 (m, 3H), 7.28−7.26 (m, 3H), 7.16 (dd, J = 7.8, 7.2 Hz, 1H), 7.07 (dd, J = 7.8, 7.2 Hz, 1H), 6.08−6.04 (m, 1H), 4.17−4.10 (m, 1H), 3.86 (s, 2H), 3.78 (s, 3H), 3.35−3.25 (m, 1H), 2.98 (d, J = 7.8 Hz, 1H), 2.60−2.51 (m, 1H), 2.44−2.32 (m, 1H); MS (ESI): m/z: 385 $[M + Na]^+$.

1-Carboxymethyl-*N*-phenylacetyl-1,3,4,9-tetrahydro-*β*-carboline (9d). To a solution of **9c** (180 mg, 0.5 mmol) in MeOH (4 mL) was injected LiOH (1.5 mmol) in H_2O (1 mL) under ice cooling, and the mixture was stirred under ice cooling for 10 min and then at rt for 3 h. The reaction mixture was treated with 10% HCl to pH = 1, extracted with EtOAc, washed with saturated brine, and dried over anhydrous Na_2SO_4. The solvent was concentrated in vacuo. The crude product was purified by gel column chromatography (eluent, $CHCl_3$:MeOH = 80:1 to 20:1) to give compound **9d** as a white solid. Yield: 68%. ^{1}H NMR (300 MHz, DMSO): δ 12.32 (br s, 1H), 10.69 (br s, 1H), 7.39−7.21 (m, 6H), 7.19−7.12 (m, 1H), 7.06−7.02 (m, 1H), 6.98−6.92 (m, 1H), 6.01−5.97 (m, 1H), 4.12−4.07 (m, 1H), 3.84 (s, 2H), 3.48−3.43 (m, 1H), 2.95−2.93 (m, 1H), 2.87−2.85 (m, 1H), 2.64−2.60 (m, 1H); MS (ESI): m/z: 347 $[M - H]^-$.

6-Fluoro-*N*-phenylacetyl-1,3,4,9-tetrahydro-*β*-carboline (10a). To a solution of phenyl acetic acid (51 mg, 0.48 mmol) in anhydrous DMF (5 mL) were added EDC (119 mg, 0.62 mmol) and HOBt (72 mg, 0.53 mmol) at 0 °C, and then 6-fluoro-1,3,4,9-tetrahydro-*β*-carboline (70 mg, 0.37 mmol) was added to the mixture after stirring for 15 min. The mixture was stirred for another 3 h, diluted with H_2O, and extracted with EtOAc (3 × 60 mL). The combined organic phase was dried over anhydrous Na_2SO_4, concentrated, and chromatographed by silica gel column chromatography (eluent, PE:EA = 6:1 to 3:1) to give 71 mg (62% yield) of compound **10a**. ^{1}H NMR (300 MHz, DMSO): δ 10.96 (br s, 1H), 7.29−7.17 (m, 6H), 7.13−7.10 (m, 1H), 6.89−6.83 (m, 1H), 4.70 (s, 2H), 3.86−3.81 (m, 4H), 2.65−2.56 (m, 2H); MS (ESI): m/z: 331 $[M + Na]^+$.

6-Bromo-*N*-phenylacetyl-1,3,4,9-tetrahydro-*β*-carboline (10b). The title compound was synthesized according to the procedure of preparing **10a** except using 6-bromo-1,3,4,9-tetrahydro-*β*-carboline instead of 6-fluoro-1,3,4,9-tetrahydro-*β*-carboline. Yield: 62%, white solid. ^{1}H NMR (300 MHz, DMSO): δ 10.84 (br s, 1H), 7.36−7.23 (m, 6H), 7.05−7.00 (m, 1H), 6.97−6.92 (m, 1H), 4.70 (s, 2H), 3.86−3.82 (m, 4H), 2.69−2.59 (m, 2H).

6-Hydroxy-1-methyl-*N*-phenylacetyl-1,3,4,9-tetrahydro-*β*-carboline (10c). To a solution of compound 6-benzoxy-1-methyl-N-phenylacetyl-1,3,4,9-tetrahydro-*β*-carboline (107 mg, 0.26 mmol) in MeOH (5 mL) was added Pd/C (10 mg, 10 wt %) under hydrogen atmosphere at room temperature for 3 h. The reaction mixture was filtered through Celite, and the solvent was concentrated in vacuo. The crude product was purified by gel column chromatography (eluent, PE:EtOAc = 4:1 to 1:1) to give compound **10c** (43 mg, 54%).^{1}H NMR (300 MHz, DMSO): δ 10.52 (br s, 1H), 8.54 (br s, 1H), 7.32−7.23 (m, 5H), 7.06 (d, J = 8.4 Hz, 1H), 6.64−6.63 (m, 1H), 6.55−6.53 (m, 1H), 5.57−5.45 (m, 1H), 4.15−4.09 (m, 1H), 3.85−3.71 (m, 1H), 3.31−3.24 (m, 1H), 2.60−2.51 (m, 1H), 2.44−2.32 (m, 1H), 1.37 (d, J = 6.9 Hz, 3H); MS (ESI): m/z: 343 $[M + Na]^+$.

SBE Luciferase Assay. The luciferase assay was performed as previously described.[26,34,35] Briefly, HaCaT cells (2.5 × 10^4 cells per well) were seeded into 24-well Corning Costar plates (Corning, NY) 24 h prior to transfection. A 200 ng amount of SBE-luc plasmid and 2 ng of pRL-CMV construct (Renilla luciferase, for transfection normalization) were transfected using LipofectamineTM 2000 (Invitrogen) in serum-free conditions for 8 h. The cells were then allowed to recover in medium containing 10% FBS for 24 h, serum-starved for another 24 h, and then treated with 5 ng/mL TGF*β*1. At the same time, samples of test compounds (1.0 μM) dissolved in 100% dimethyl sulfoxide (DMSO) were added in triplicate wells. Within 24 h, cells were lysed and tested in a dual-luciferase assay (Promega Inc., Fitchburg, WI).

Cell Proliferation Assay (Sulforhodamine B, SRB). Cells were seeded in 96-well plates at 1 × 10^4 per well. After incubation with tested compounds for 48 h, cell monolayers were fixed with 10% (w/v) trichloroacetic acid (TCA) and stained for 30 min in room temperature. After washing repeatedly with 1% (v/v) acetic acid, we used 10 mM Tris base solution to dissolve the protein-bound dye for OD determination at 510 nm using a microplate reader. The decrease in SRB absorbance as a percentage of DMSO control well absorbance was taken as the percentage of proliferation inhibition by a given compound tested.

Wound Healing Assay. Cells were seeded onto sterile 12-well plates and incubated at 37 °C in complete RPMI 1640 medium to 100% confluence for the experiment and then changed to fresh serum-free media for another 12 h. Wounds were created in cells using a sterile 10.0 μL pipet tip. The cells were washed twice with PBS, and the media in each well was replaced with 1 mL complete RPMI 1640. The compounds at specified concentrations were added to each well, and the cells were incubated at 37 °C for 24 h under complete conditions. Cell migration was observed and photomicrographed for quantitation and image analysis of each treatment.

Transwell Migration Assay. Cells (5 × 10^5) in 400 μL of DMEM medium were seeded into each transwell chamber with filter membranes of 8 μm pore size (Millipore, Schwalbach, Germany). Fresh medium (600 μL, containing 10% FBS) was added to the bottom chamber, and cells were allowed to attach to the insets at 37 °C and 5% CO_2 in a humidified incubator. Following 12−24 h incubation, nonmigrated cells were removed with cotton swabs, while migrated cells on the lower surface of membranes were fixed and stained with 0.2% crystal violet in phosphate-buffered saline (PBS) at room temperature. Migrated cells were counted in five randomly chosen 10× magnification fields per membrane under an Olympus inverted microscope.

Cell Motility. H1299 cells (5 × 10^4) were seeded in 30 mm cell culture dishes and pretreated with or without compound **8d** for 24 h. Cells motility was monitored with Olympus Time-lapse workstation (Olympus X71, 1 picture per 10 min, total time of 10 h). All pictures were then processed with Image Pro-Plus 6.0, and statistical analysis performed using Microsoft Office software.

Xenograft Model of Lung Cancer. Five week old nude mice were allowed to acclimate for a week before inoculation with A549 tumor cells. An amount of 5 × 10^5 cells prepared in PBS was injected subcutaneously. When the tumor reached a diameter of about 10 mm, 15 mice were matched according to tumor size and randomly divided into three groups: control group, compound **8d** (5.0 mg/kg/day) group, and gefitinib (20 mg/kg/day) dose group, respectively. All mice were intraperitoneally injected with compound **8d** (5.0 mg/kg) or gefitinib (20 mg/kg) in 50 μL of DMSO every day, and an equivalent volume of DMSO was injected into control mice (n = 5). Mice were treated consecutively for 60 days, and the body weight and the tumor dimensions were measured daily. The volume of the tumor was calculated as volume equals 0.52 × AB^2, where A is the long axis and B is the short axis.

Orthotopic Xenograft Model of Breast Cancer. An amount of 5 × 10^4 4T1-luciferase mouse breast cancer cells was injected into the mammary fat pads of six week old Balb/c female mice. After 7 days

dx.doi.org/10.1021/jm401117t | J. Med. Chem. 2014, 57, 600−612

when orthotopic tumors had grown to a diameter of about 5 mm, 24 mice were randomly divided into three groups according to orthotopic tumor size: control group, **8d** (1.0 mg/kg/d) dose group, and **8d** (5.0 mg/kg/d) dose group, respectively. Treatment group mice were intraperitoneally injected with the appropriate dose, whereas the control group mice were injected with same amount of solvent (DMSO). The body weight of mice was measured daily before injecting with compound **8d**. Following 20 days of treatment, breast cancer cells in mice were evaluated by the use of in vivo imaging (IVIS).[34]

Molecular Docking Modeling Assay. The docking assay experiments were carried out as previously described by our research group.[26] The X-ray crystal structure of TGFRβI (PDB ID: 3TZM) was obtained from the Protein Data Bank (PDB) (www.rcsb.org/).[36] The missing residues of the crystal structure were fixed by using Modeller9v8.[37] For optimization of the fixed protein, the temperature of the optimization was set at 300 K, and the cycle of the optimization was 10. All the small molecule structures were built and energy was minimized using the Chemoffice software package. Autodock 4.2 version (developed by the Scripps Research Institute and Olson lab) was used for corresponding docking experiments. All of the water molecules were removed prior to modeling experiments. The active site was chosen from those within the primary ligand binding pocket in the PDB files. The picture was prepared with UCSF Chimera 1.8. To distinguish different compounds, we depicted the carbon skeleton with different colors.

For the virtual screening of the TGFβRI kinase inhibitors, first of all, the molecular library (derived from ChemDiv Company as well as our laboratory) was screened by UCSF DOCK6.5 and scored by GRID. The result was screened with a cutoff GRID score of less than −60. This yielded about 40 000 molecules for the next step. The secondary library was screened by Autodock vina v1.1 and scored by free energy. For the method of vina screening, the exhaustiveness was equal to 64, the size of the box was (40, 36, 32), and num_mode = 10. Following the screening of Autodock vina, we used a cutoff of free energy score of less than −11.3 kcal/mol to generate the penultimate molecular library. This molecular library was finally screened by UCSF DOCK6.5 amber score to generate the final candidates. We used the default operation parameter and set the cutoff of the UCSF DOCK6.5 amber score at less than −20.00.

■ ASSOCIATED CONTENT

Supporting Information

Hydrophobicity surface of the X-ray crystal structure of TGFβRI kinase domain (PDB ID: 3TZM) interacted with **3**, and the effect of compound **8d** on the EGF-induced migration of H1299 lung cancer cells. This material is available free of charge via the Internet at http://pubs.acs.org.

■ AUTHOR INFORMATION

Corresponding Authors

*Phone: +86-21-2420-6647. Fax: +86-21-5434-4922. E-mail: yhchen@bio.ecnu.edu.cn.

*E-mail: jluo@bio.ecnu.edu.cn.

*E-mail: myliu@bio.ecnu.edu.cn.

Author Contributions

#These authors contributed equally to this work.

Notes

The authors declare no competing financial interest.

■ ACKNOWLEDGMENTS

We thank Stefan Siwko for comments and advice. This work was partially supported by the grants from National Basic Research Program of China (2012CB910404), National Major Scientific and Technological Special Project for "Significant New Drugs Development" (2013ZX09507001), National Natural Science Foundation of China (81202407, 81272911), The Science and Technology Commission of Shanghai Municipality (11DZ2260300), Research Fund for the Doctoral Program of Higher Education of China (20120076120029), and the Fundamental Research Funds for the Central Universities (78210048).

■ ABBREVIATIONS USED

TGFβ, transforming growth factor-β; EMTs, epithelial−mesenchymal transitions; EDC, *N*-(3-dimethylaminopropyl)-*N*′-ethylcarbodiimide hydrochloride; HOBt, 1-hydroxybenzotriazole; SBE, Smad binding element; HATU, *O*-(7-azabenzotriazol-1-yl)-*N*,*N*,*N*′,*N*′-tetramethyluronium hexafluorophosphate; CDI, *N*,*N*′-carbonyldiimidazole; PE, petroleum ether; EA, ethyl acetate; NSCLC, nonsmall-cell lung carcinoma; PC-9, human lung adenocarcinoma cells; A549, human lung adenocarcinome cells; H1299 (also as NCI-H1299), human nonsmall cell lung carcinoma cells; SAR, structure−activity relationship; 4T1, mouse mammary tumor cell line

■ REFERENCES

(1) Siegel, R.; Naishadham, D.; Jemal, A. Cancer statistics, 2013. *Ca-Cancer J. Clin.* **2013**, *63*, 11−30.

(2) Siegel, R.; Naishadham, D.; Jemal, A. Cancer statistics, 2012. *Ca-Cancer J. Clin.* **2012**, *62*, 10−29.

(3) Chen, L.; Yang, S.; Jakoncic, J.; Zhang, J. J.; Huang, X. Y. Migrastatin analogues target fascin to block tumour metastasis. *Nature* **2010**, *464*, 1062−1066.

(4) Mehlen, P.; Puisieux, A. Metastasis: a question of life or death. *Nat. Rev. Cancer* **2006**, *6*, 449−458.

(5) Levy, L.; Hill, C. S. Alterations in components of the TGF-beta superfamily signaling pathways in human cancer. *Cytokine Growth Factor Rev.* **2006**, *17*, 41−58.

(6) Miyazono, K.; Kusanagi, K.; Inoue, H. Divergence and convergence of TGF-beta/BMP signaling. *J. Cell Physiol.* **2001**, *187*, 265−276.

(7) Leask, A.; Abraham, D. J. TGF-beta signaling and the fibrotic response. *FASEB J.* **2004**, *18*, 816−827.

(8) Agrotis, A.; Kalinina, N.; Bobik, A. Transforming growth factor-beta, cell signaling and cardiovascular disorders. *Curr. Vasc. Pharmacol.* **2005**, *3*, 55−61.

(9) Bierie, B.; Moses, H. L. Tumour microenvironment: TGFbeta: the molecular Jekyll and Hyde of cancer. *Nat. Rev. Cancer* **2006**, *6*, 506−520.

(10) Eichhorn, P. J.; Rodon, L.; Gonzalez-Junca, A.; Dirac, A.; Gili, M.; Martinez-Saez, E.; Aura, C.; Barba, I.; Peg, V.; Prat, A.; Cuartas, I.; Jimenez, J.; Garcia-Dorado, D.; Sahuquillo, J.; Bernards, R.; Baselga, J.; Seoane, J. USP15 stabilizes TGF-beta receptor I and promotes oncogenesis through the activation of TGF-beta signaling in glioblastoma. *Nat. Med.* **2012**, *18*, 429−435.

(11) Li, H. Y.; McMillen, W. T.; Heap, C. R.; McCann, D. J.; Yan, L.; Campbell, R. M.; Mundla, S. R.; King, C. H.; Dierks, E. A.; Anderson, B. D.; Britt, K. S.; Huss, K. L.; Voss, M. D.; Wang, Y.; Clawson, D. K.; Yingling, J. M.; Sawyer, J. S. Optimization of a dihydropyrrolopyrazole series of transforming growth factor-beta type I receptor kinase domain inhibitors: Discovery of an orally bioavailable transforming growth factor-beta receptor type I inhibitor as antitumor agent. *J. Med. Chem.* **2008**, *51*, 2302−2306.

(12) Nagaraj, N. S.; Datta, P. K. Targeting the transforming growth factor-beta signaling pathway in human cancer. *Expert Opin. Investig. Drugs* **2010**, *19*, 77−91.

(13) Schade, D.; Lanier, M.; Willems, E.; Okolotowicz, K.; Bushway, P.; Wahlquist, C.; Gilley, C.; Mercola, M.; Cashman, J. R. Synthesis and SAR of b-annulated 1,4-dihydropyridines define cardiomyogenic compounds as novel inhibitors of TGFbeta signaling. *J. Med. Chem.* **2012**, *55*, 9946−9957.

(14) Shimizu, T.; Kimura, K.; Sakai, T.; Kawakami, K.; Miyazaki, T.; Nakouji, M.; Ogawa, A.; Ohuchi, H.; Shimizu, K. Synthesis and evaluation of [2-(4-quinolyloxy)phenyl]methanone derivatives: Novel selective inhibitors of transforming growth factor-beta kinase. *J. Med. Chem.* **2008**, *51*, 3326−3329.
(15) Goldberg, F. W.; Ward, R. A.; Powell, S. J.; Debreczeni, J. E.; Norman, R. A.; Roberts, N. J.; Dishington, A. P.; Gingell, H. J.; Wickson, K. F.; Roberts, A. L. Rapid generation of a high quality lead for transforming growth factor-beta (TGF-beta) type I receptor (ALK5). *J. Med. Chem.* **2009**, *52*, 7901−7905.
(16) Kim, D. K.; Jang, Y.; Lee, H. S.; Park, H. J.; Yoo, J. Synthesis and biological evaluation of 4(5)-(6-alkylpyridin-2-yl)imidazoles as transforming growth factor-beta type 1 receptor kinase inhibitors. *J. Med. Chem.* **2007**, *50*, 3143−3147.
(17) Akhurst, R. J.; Hata, A. Targeting the TGFbeta signalling pathway in disease. *Nat. Rev. Drug Discovery* **2012**, *11*, 790−811.
(18) Wang, G.; Jia, S.; Wang, T.; Chen, L.; Song, Q.; Li, W. Effect of ferrous ion on epsilon-poly-L-lysine biosynthesis by Streptomyces diastatochromogenes CGMCC3145. *Curr. Microbiol.* **2011**, *62*, 1062−1067.
(19) Uhl, M.; Aulwurm, S.; Wischhusen, J.; Weiler, M.; Ma, J. Y.; Almirez, R.; Mangadu, R.; Liu, Y. W.; Platten, M.; Herrlinger, U.; Murphy, A.; Wong, D. H.; Wick, W.; Higgins, L. S.; Weller, M. SD-208, a novel transforming growth factor beta receptor I kinase inhibitor, inhibits growth and invasiveness and enhances immunogenicity of murine and human glioma cells in vitro and in vivo. *Cancer Res.* **2004**, *64*, 7954−7961.
(20) Saunier, E. F.; Akhurst, R. J. TGF beta inhibition for cancer therapy. *Curr. Cancer Drug Targets* **2006**, *6*, 565−578.
(21) Hjelmeland, M. D.; Hjelmeland, A. B.; Sathornsumetee, S.; Reese, E. D.; Herbstreith, M. H.; Laping, N. J.; Friedman, H. S.; Bigner, D. D.; Wang, X. F.; Rich, J. N. SB-431542, a small molecule transforming growth factor-beta-receptor antagonist, inhibits human glioma cell line proliferation and motility. *Mol. Cancer Ther.* **2004**, *3*, 737−745.
(22) de Gouville, A. C.; Boullay, V.; Krysa, G.; Pilot, J.; Brusq, J. M.; Loriolle, F.; Gauthier, J. M.; Papworth, S. A.; Laroze, A.; Gellibert, F.; Huet, S. Inhibition of TGF-beta signaling by an ALK5 inhibitor protects rats from dimethylnitrosamine-induced liver fibrosis. *Br. J. Pharmacol.* **2005**, *145*, 166−177.
(23) Suzuki, E.; Kim, S.; Cheung, H. K.; Corbley, M. J.; Zhang, X.; Sun, L.; Shan, F.; Singh, J.; Lee, W. C.; Albelda, S. M.; Ling, L. E. A novel small-molecule inhibitor of transforming growth factor beta type I receptor kinase (SM16) inhibits murine mesothelioma tumor growth in vivo and prevents tumor recurrence after surgical resection. *Cancer Res.* **2007**, *67*, 2351−2359.
(24) Yingling, J. M.; Blanchard, K. L.; Sawyer, J. S. Development of TGF-beta signalling inhibitors for cancer therapy. *Nat. Rev. Drug Discovery* **2004**, *3*, 1011−1022.
(25) Roth, G. J.; Heckel, A.; Brandl, T.; Grauert, M.; Hoerer, S.; Kley, J. T.; Schnapp, G.; Baum, P.; Mennerich, D.; Schnapp, A.; Park, J. E. Design, synthesis, and evaluation of indolinones as inhibitors of the transforming growth factor beta receptor I (TGFbetaRI). *J. Med. Chem.* **2010**, *53*, 7287−7295.
(26) Fang, Y.; Chen, Y.; Yu, L.; Zheng, C.; Qi, Y.; Li, Z.; Yang, Z.; Zhang, Y.; Shi, T.; Luo, J.; Liu, M. Inhibition of breast cancer metastases by a novel inhibitor of TGFbeta receptor 1. *J. Natl. Cancer Inst.* **2013**, *105*, 47−58.
(27) Wu, T. Y.; Schultz, P. G. A versatile linkage strategy for solid-phase synthesis of *N*,*N*-dimethyltryptamines and *β*-carbolines. *Org. Lett.* **2002**, *4*, 4033−4036.
(28) Luis, S. V.; Burguete, M. I. The Fischer indole synthesis of 8-methyl-5-substituted-1-oxo-*β*-carbolines: A remarkable high yield of a [1,2]-methyl migration. *Tetrahedron* **1991**, *47*, 1737−1744.
(29) Lehmann, J.; Pohl, U. Indoles. VI. Lactamization of 4,9-dihydropyrano[3,4-b]indol-1(3H)-ones with methylamine. A new synthetic route to strychnocarpine and its derivatives. *Arch. Pharm. (Weinheim, Ger.)* **1988**, *321*, 411−414.
(30) Liu, J.; Jiang, X.; Zhao, M.; Zhang, X.; Zheng, M.; Peng, L.; Peng, S. A class of 3*S*-2-aminoacyltetrahydro-*β*-carboline-3-carboxylic acids: Their facile synthesis, inhibition for platelet activation, and high in vivo antithrombotic potency. *J. Med. Chem.* **2010**, *53*, 3106−3116.
(31) Yachida, S.; Jones, S.; Bozic, I.; Antal, T.; Leary, R.; Fu, B.; Kamiyama, M.; Hruban, R. H.; Eshleman, J. R.; Nowak, M. A.; Velculescu, V. E.; Kinzler, K. W.; Vogelstein, B.; Iacobuzio-Donahue, C. A. Distant metastasis occurs late during the genetic evolution of pancreatic cancer. *Nature* **2010**, *467*, 1114−1117.
(32) Wells, A.; Grahovac, J.; Wheeler, S.; Ma, B.; Lauffenburger, D. Targeting tumor cell motility as a strategy against invasion and metastasis. *Trends Pharmacol. Sci.* **2013**, *34*, 283−289.
(33) Palmer, T. D.; Ashby, W. J.; Lewis, J. D.; Zijlstra, A. Targeting tumor cell motility to prevent metastasis. *Adv. Drug Delivery Rev.* **2011**, *63*, 568−581.
(34) Alex, A.; Natalia, K.; Alex, B. Transforming Growth Factor-beta, Cell Signaling and Cardiovascular Disorders. *Curr. Vasc. Pharmacol.* **2005**, *3*, 55−61.
(35) Luo, J.; Zhou, W.; Zhou, X.; Li, D.; Weng, J.; Yi, Z.; Cho, S. G.; Li, C.; Yi, T.; Wu, X.; Li, X. Y.; de Crombrugghe, B.; Höök, M.; Liu, M. Regulation of bone formation and remodeling by G-protein-coupled receptor 48. *Development* **2009**, *136*, 2747−2756.
(36) Fiser, A.; Do, R. K.; Sali, A. Modeling of loops in protein structures. *Protein Sci.* **2000**, *9*, 1753−1773.
(37) Ogunjimi, A. A.; Zeqiraj, E.; Ceccarelli, D. F.; Sicheri, F.; Wrana, J. L.; David, L. Structural basis for specificity of TGF*β* family receptor small molecule inhibitors. *Cell. Signal.* **2011**, *24*, 476−483.